articles

molecular pharmaceutics

Bimodal Effect of Hypoxia in Cancer: Role of Hypoxia Inducible Factor in Apoptosis

Yang Wang, Refika I. Pakunlu, William Tsao, Vitaly Pozharov, and Tamara Minko*

Department of Pharmaceutics, Ernest Mario School of Pharmacy, Rutgers, The State University of New Jersey, Piscataway, New Jersey 08854

Received December 8, 2003

Abstract: The effects of the separate and combined application of hypoxia and antisense oligonucleotides (ASO) against hypoxia inducible factor 1α (HIF1A) on cancer cells were examined. Experiments were carried out on human ovarian carcinoma cells in four series: (1) control [Normoxia (5% CO_2 in air), no treatment], (2) hypoxia (1% O_2, 5% CO_2, and 94% N_2 for 48 h), (3) treatment with ASO targeted to HIF1A (48 h), and (4) combined action of hypoxia and ASO. After treatment, the following processes and factors were monitored: apoptosis, cellular metabolism and viability, expression of genes encoding HIF1A, von Hippel-Lindau tumor suppressor protein (VHL), and genes responsible for cell death induction and antiapoptotic defense (P53, BCL2, BAX, and caspases 9 and 3). Expression of caspase 9 and HIF1A protein was confirmed by Western blotting. Liposomes were used as a delivery system of HIF1A ASO. It was found that hypoxia alone significantly disturbed cellular metabolism, reducing the level of respiration by 50% when compared with control. Hypoxia induced apoptosis by upregulating the P53-, BAX-, and caspase-dependent cell death pathways, while activating cellular antiapoptotic defense by the overexpression of BCL2 protein. Both opposing effects were dependent on the overexpression of hypoxia inducible factor. We conclude that hypoxia induces a bimodal effect, simultaneously promoting cell death and activating cellular resistance. The downregulation of HIF1A promoted cell death induction and prevented activation of cellular defense by hypoxia. This suggests that HIF1A is a potential candidate for anticancer therapeutic targeting.

Keywords: Liposomal delivery; antisense oligonucleotides; hypoxia inducible factor 1α; hypoxia; cancer; apoptosis

Introduction

Hypoxia, a reduction in tissue oxygen tension, induces a wide spectrum of effects in different tissues and systems of organisms, triggering cell injury and death and simultaneously activating systemic and cellular compensative mechanisms.[1,2] If the negative effects of hypoxia overcome the compensatory mechanisms, hypoxia will result in the disturbances of cellular metabolism and the failure of different vital functions and finally will lead to cellular and organismal death.[3−6]

Hypoxia occurs in solid tumors due to the attenuated oxygen supply resulting from the exponential cellular

* To whom correspondence should be addressed: Department of Pharmaceutics, Ernest Mario School of Pharmacy, Rutgers, The State University of New Jersey, 160 Frelinghuysen Rd., Piscataway, NJ 08854-8020. Phone: (732) 445-3831. Fax: (732) 445-3134. E-mail: minko@cop.rutgers.edu.

(1) Minko, T.; Stefanov, A.; Pozharov, V. Lung hypoxia: antioxidant and antiapoptotic effects of liposomal α-tocopherol. *J. Appl. Physiol*. **2002**, *93*, 1550−1560.
(2) Seta, K. A.; Spicer, Z.; Yuan, Y.; Lu, G.; Millhorn, D. E. Responding to hypoxia: lessons from a model cell line. *Sci. STKE* **2002**, *20*, RE11.
(3) Brunelle, J. K.; Chandel, N. S. Oxygen deprivation induced cell death: an update. *Apoptosis* **2002**, *7*, 475−482.

10.1021/mp034031n CCC: $27.50
Published on Web 02/04/2004

proliferation accompanied by a linear increase in vascular supply.[7,8] Hypoxic induction of death in tumor cells can potentially be used in cancer treatment.[9] The use of hypoxia-induced cell damage in cancer therapy is countered by the development of a cell's adaptive responses. We hypothesize that the suppression of compensatory adaptation during cancer therapy can significantly increase the efficacy of the treatment.

Hypoxia inducible factor 1 (HIF1) is a transcription factor found in mammalian cells cultured under reduced oxygen tension that plays an essential role in cellular and systemic homeostatic responses to hypoxia.[10−13] HIF1 is a heterodimer composed of a 120 kDa HIF1 α subunit complexed with a 91−94 kDa HIF1 β subunit. HIF1 plays a key role in the cellular response to hypoxia, including the regulation of genes involved in energy metabolism, angiogenesis, and apoptosis. The α subunits of HIF are rapidly degraded by the proteasome under normal conditions but are stabilized by hypoxia. Upregulation of HIF1A induces the expression of different genes whose products play both adaptive and damaging roles in the cellular response to hypoxia. Therefore, this gene might play a bimodal role in the cellular hypoxic response, inducing opposite effects of hypoxia: an initial increase in resistance followed by cell death under sustained hypoxia.[13] Consequently, HIF and other elements of signaling pathways of hypoxia can be promising candidates for therapeutic targeting. However, the use of such targets is limited by the incomplete knowledge of physiological and pathological effects of hypoxia on cancer cells and the role of hypoxia inducible factor in the development of cellular damage and resistance in particular. This paper is aimed at investigating the effects of hypoxia on induction of death and resistance in cancer cells and especially focuses on the role of HIF1A in this process.

Experimental Section

Cell Culture. The human ovarian carcinoma A2780 cell line was obtained from T. C. Hamilton (Fox Chase Cancer Center, Philadelphia, PA). Cells were cultured in RPMI 1640 medium (Sigma Chemical Co., St. Louis, MO) supplemented with 10% fetal bovine serum (HyClone, Logan, UT). All experiments were performed with cells in the exponential growth phase.

Hypoxia Model. Cells were maintained at 37 °C in a humidified incubator containing 21% O_2 and 5% CO_2 in air (termed normoxic conditions). Hypoxia was produced by placing cell culture plates in a modular incubator chamber (Billupus-Rottemberg Inc., Del Mar, CA) and then flushing the chamber with a mixture of 1% O_2, 5% CO_2, and 94% nitrogen at a flow rate of 3 L/min for 15 min.[14] The chamber was sealed and kept at 37 °C for 48 h. The flushing procedure was repeated every 12 h.

Liposomal Delivery of Antisense Oligonucleotides Targeted to HIF1A. The sequences of the antisense and sense HIF1A oligonucleotides were 5′-GCC GGC GCC CTC CAT-3′ and 5′-ATG GAG GGC GCC GGC-3′, respectively.[15] The DNA backbone of all bases in oligonucleotides was P-ethoxy modified to enhance the nuclease resistance and increase the efficacy of incorporation into liposomes. Antisense oligonucleotides (ASO) were synthesized by Oligos Etc. (Wilsonville, OR). ASO were packaged in liposomes, which were prepared using the previously described lipid film rehydration method.[1,16] Briefly, lipids (Avanti Polar Lipids, Alabaster, AL) were dissolved in chloroform, evaporated to a thin film in a rotary evaporator, and rehydrated with citrate buffer. The lipid ratio for all formulations was 7:3:10 (egg phosphatidylcholine:1,2-dipalmitoyl-*sn*-glycero-3-phosphatidylcholine:cholesterol). ASO were loaded into the liposomes by dissolving the ASO in the rehydration buffer at a concentration of 0.5 mM. The encapsulation efficacy ranged from 51.5 to 58.3% in different series of experiments. The mean liposome diameter was ∼100 nm.

Release of ASO from Liposomes and Intracellular Localization. To analyze release of ASO from liposomes and their intracellular localization, a portion of oligonucleo-

(4) Grow, J.; Barks, J. D. Pathogenesis of hypoxic-ischemic cerebral injury in the term infant: current concepts. *Clin. Perinatol.* **2002**, *29*, 585−602.
(5) Ikeda, K.; Negishi, H.; Yamori, Y. Antioxidant nutrients and hypoxia/ischemia brain injury in rodents. *Toxicology* **2003**, *189*, 55−61.
(6) Lyn, D.; Lui, X.; Bennett, N. A.; Bao, S. Ischemia elicits a coordinated expression of apoptotic proteins in mouse myocardium. *Sci. World J.* **2001**, *1*, 39.
(7) Harris, A. L. Hypoxia: a key regulatory factor in tumour growth. *Nat. Rev. Cancer* **2002**, *2*, 38−47.
(8) Shannon, A. M.; Bouchier-Hayes, D. J.; Condron, C. M.; Toomey, D. Tumour hypoxia, chemotherapeutic resistance and hypoxia-related therapies. *Cancer Treat. Rev.* **2003**, *29*, 297−307.
(9) Brown, J. M. Tumor microenvironment and the response to anticancer therapy. *Cancer Biol. Ther*. **2002**, *1*, 453−458.
(10) Bickler, P. E.; Donohoe, P. H. Adaptive responses of vertebrate neurons to hypoxia. *J. Exp. Biol.* **2002**, *205*, 3579−3586.
(11) Brune, B.; von Knethen, A.; Sandau, K. B. Transcription factors p53 and HIF-1α as targets of nitric oxide. *Cell. Signalling* **2001**, *13*, 525−533.
(12) Kietzmann, T.; Knabe, W.; Schmidt-Kastner, R. Hypoxia and hypoxia-inducible factor modulated gene expression in brain: involvement in neuroprotection and cell death. *Eur. Arch. Psychiatry Clin. Neurosci.* **2001**, *251*, 170−178.
(13) Piret, J. P.; Mottet, D.; Raes, M.; Michiels, C. Is HIF-1α a pro- or an anti-apoptotic protein? *Biochem. Pharmacol.* **2002**, *64*, 889−892.
(14) Rapisarda, A.; Uranchimeg, B.; Scudiero, D. A.; Selby, M.; Sausville, E. A.; Shoemaker, R. H.; Melillo, G. Identification of small molecule inhibitors of hypoxia-inducible factor 1 transcriptional activation pathway. *Cancer Res.* **2002**, *62*, 4316−4324.
(15) Caniggia, I.; Mostachfi, H.; Winter, J.; Gassmann, M.; Lye, S. J.; Kuliszewski, M.; Post, M. Hypoxia-inducible factor-1 mediates the biological effects of oxygen on human trophoblast differentiation through TGFβ(3). *J. Clin. Invest.* **2000**, *105*, 577−587.
(16) Pakunlu, R. I.; Cook, T. J.; Minko, T. Simultaneous modulation of multidrug resistance and antiapoptotic cellular defense by MDR1 and BCL-2 targeted antisense oligonucleotides enhances the anticancer efficacy of doxorubicin. *Pharm. Res*. **2003**, *20*, 351−359.

tides were labeled with fluorescein isothiocyanate (FITC) prior to the incorporation into the liposomes. The labeling was performed by Oligos Etc. The fluorescence of labels inside liposomes is quenched by the outer membranes of the liposomes.[17] Therefore, the intensity of FITC fluorescence is proportional to the concentration of free ASO released from the liposomes. The ASO release from liposomes in saline was monitored for 2 weeks. The fluorescence in aliquots of the incubation solution was measured every hour during the first day and once per day for the next 13 days with a fluorescent microtiter plate reader. Intracellular localization and release of ASO were studied by fluorescence microscopy. In these experiments, cell nuclei were additionally stained with Hoechst 33258 nuclear dye (Sigma). To quantitatively estimate the release of ASO, images form the fluorescence microscope were digitally photographed after incubation of cells with liposomal ASO for 7, 15, 30, and 45 min and 1, 2, 3, 24, and 48 h. Visible light and fluorescent images were simultaneously recorded for each field. The total fluorescence intensity of each field was then calculated and normalized to the total optical density of visible light images. This allowed us to take into account the number of cells in the field. These normalized intensities were then plotted against time to characterize the release of ASO inside the cells.

Aerobic and Anaerobic Metabolism. The activity of aerobic mitochondrial metabolism was estimated by a modified MTT [3-(4,5-dimethylthiazol-2-yl)-2,5-diphenyltetrazolium bromide] (Sigma) assay as previously described.[18] Briefly, cells were seeded into a 96-well microtiter plate at a density of 10 000 cells per well. Twenty-four hours after the plate had been prepared, the medium was aspirated and fresh medium containing liposomal ASO, liposomal sense oligonucleotides, empty liposomes, or an equivalent volume of saline was added, each to separate experimental plates. Separate parallel sets were then cultured under normoxic or hypoxic conditions for up to 48 h before the MTT assay was performed. In this assay, MTT is cleaved by the succinate-tetrazolium reductase system (EC 1.3.99.1) which belongs to the mitochondrial respiratory chain. Therefore, the optic density measured in this assay is proportional to the activity of oxidative pathways of mitochondrial respiration. To characterize the cell anaerobic metabolism, the concentration of lactic acid in cell lysates was measured with enzymatic assay kit 755-10 (Sigma) and was expressed per gram of protein determined using the bicinchoninic acid (BCA) protein assay kit (Pierce, Rockford, IL).

Gene Expression. Reverse transcriptase polymerase chain reaction (RT-PCR) was used for the analysis of gene expression as previously described.[19−21] Total cellular RNA was isolated using an RNeasy kit (Qiagen, Valencia, CA). First-strand cDNA was synthesized with Ready-To-Go You-Prime First-Strand Beads (Amersham Biosciences, Piscataway, NJ) with 1 μg of total cellular RNA (from 10^7 cells) and 100 ng of random hexadeoxynucleotide primer (Amersham Biosciences). After synthesis, the reaction mixture was immediately subjected to PCR, which was carried out using GenAmp PCR System 2400 (Perkin-Elmer, Shelton, CT). The pairs of primers used to amplify each type of cDNA are given in Table 1. β_2-Microglobulin (β_2-m) was used as an internal standard. The PCR regimen was as follows: 94 °C for 4 min, 55 °C for 1 min, and 72 °C for 1 min for one cycle; 94 °C for 1 min, 55 °C for 50 s, and 72 °C for 1 min for 28 cycles; and 60 °C for 10 min. PCR products were separated in 4% NuSieve 3:1 Reliant agarose gels (BMA, Rockland, ME) in 1× TBE buffer [0.089 M Tris-borate and 0.002 M EDTA (pH 8.3); Research Organics Inc., Cleveland, OH] by submarine electrophoresis. The gels were stained with ethidium bromide, digitally photographed, and scanned using Gel Documentation System 920 (NucleoTech, San Mateo, CA). The extent of gene expression was calculated as the ratio of the mean band density of the analyzed RT-PCR product to that of the internal standard (β_2-m).

Table 1. List of Primers Used in RT-PCR

Genes	Primers (5' to 3')	
	Sense primer	Antisense primer
HIF1A	cacagaaatggccttgtgaa	ccaagcaggtcataggtggt
VHL	ggtcacctttggctcttcag	tgacgatgtccagtctcctg
P53	gaagacccaggtccagatga	ggtaggttttctgggaaggg
BAX	tttgcttcagggtttcatcc	gccactcggaaaaagacctc
BCL2	ggattgtggccttctttgag	ccaaactgagcagagtcttc
Caspase 3	tggaattgatgcgtgatgtt	ggcaggcctgaataatgaaa
Caspase 9	tgactgccaagaaaatggtg	cagctggtcccattgaagat
β_2-*m* (Internal standard)	acccccactgaaaaagatga	atcttcaaacctccatgatg

Protein Expression. To confirm RT-PCR data, the expression of HIF1A and caspase 9 was assessed. The identification of these proteins was achieved by Western immunoblotting analysis and processed using scanning densitometry to quantify the expressed protein. To this end, harvested cells were lysed in Ripa buffer (Santa Cruz Biotechnologies, Inc., Santa Cruz, CA) using a needle and syringe. Following incubation on ice for 45 min, the cells were centrifuged at 10000*g* for 10 min. Protein content in the supernatant was determined using the BCA protein assay kit (Pierce), and 50 μg of protein was run on a 15% sodium

(17) Tsukioka, Y.; Matsumura, Y.; Hamaguchi, T.; Koike, H.; Moriyasu, F.; Kakizoe, T. Pharmaceutical and biomedical differences between micellar doxorubicin (NK911) and liposomal doxorubicin (Doxil). *Jpn. J. Cancer Res.* **2002**, *93*, 1145−1153.

(18) Minko, T.; Kopeckova, P.; Kopecek, J. Chronic exposure to HPMA copolymer bound adriamycin does not induce multidrug resistance in a human ovarian carcinoma cell line. *J. Controlled Release* **1999**, *59*, 133−148.

(19) Minko, T.; Kopeckova, P.; Kopecek, J. Efficacy of the chemotherapeutic action of HPMA copolymer-bound doxorubicin in a solid tumor model of ovarian carcinoma. *Int. J. Cancer* **2000**, *86*, 108−117.

(20) Minko, T.; Dharap, S. S.; Fabbricatore, A. T. Enhancing the efficacy of chemotherapeutic drugs by the suppression of anti-apoptotic cellular defense. *Cancer Detect. Prev.* **2003**, *27*, 193−202.

(21) Appenzeller, O.; Minko, T.; Pozharov, V.; Bonfichi, M.; Malcovati, L.; Gamboa, J.; Bernardi, L. Gene expression in the Andes and neurology at sea level. *J. Neurol. Sci.* **2003**, *207*, 37−41.

dodecyl sulfate (SDS)−polyacrylamide gel immersed in Tris-glycine-SDS buffer (Bio-Rad, Hercules, CA) for 90 min at 70 V. Proteins were transferred to an Immobilon-P nitrocellulose membrane (Millipore, Bedford, MA) in Tris-glycine buffer (Bio-Rad) for 90 min at 100 V. The membrane was blocked in nonfat milk for 2 h at room temperature on a rotating shaker to prevent nonspecific binding, washed, and incubated overnight with an anti-HIF1A mouse primary antibody (1:100 dilution, Lab Vision Corp., Fremont, CA) and an anti-caspase 9 rabbit primary antibody (1:2000 dilution, Stress Gen Biotechnologies, Victoria State, BC,) at 4 °C. Following further washing, the membrane was immersed in goat anti-rabbit and goat anti-mouse IgG biotinylated antibodies (1:3000 and 1:1000 dilutions, respectively; Bio-Rad) at room temperature for 1.5 h on a rotating shaker. Bands were visualized using an alkaline phosphatase color development reagent (Bio-Rad). The bands were digitally photographed and scanned using Gel Documentation System 920 (NucleoTech).

Caspase 3 Activity. The direct measurements of caspase 3 activity were made using a colorimetric protease assay kit (MBL International, Watertown, MA) as previously described.[16] The assay is based on the spectrophotometric detection of the chromophore *p*-nitroanilide (pNA) after cleavage from the X−pNA substrates, where X stands for an amino acid sequence recognized by the specific caspase (DEVD for caspases 3). The increase in the caspase activity was determined by comparing these results with the level of the untreated control incubated with saline.

Apoptosis. Two approaches were used to assess the induction of apoptosis. The first approach was based on measuring the enrichment of histone-associated DNA fragments (mono- and oligonucleosomes) in the cell cytoplasm using anti-histone and anti-DNA antibodies with a cell death detection ELISA Plus kit (Roche, Nutley, NJ) as previously described.[22,23] The second approach was based on the detection of single- and double-stranded DNA breaks (nicks) with an in situ cell death detection kit (Roche) using the terminal deoxynucleotidyl transferase-mediated dUTP-fluorescein nick end labeling (TUNEL) method as previously described.[22,23] Briefly, cells were fixed, permeabilized, and incubated with the TUNEL reaction mixture. The label incorporated at the damaged sites of the DNA was visualized with a fluorescence microscope.

Statistical Analysis. Data were analyzed using descriptive statistics and single-factor analysis of variance (ANOVA) and presented as the mean value ± the standard deviation (SD) from four to eight independent measurements.

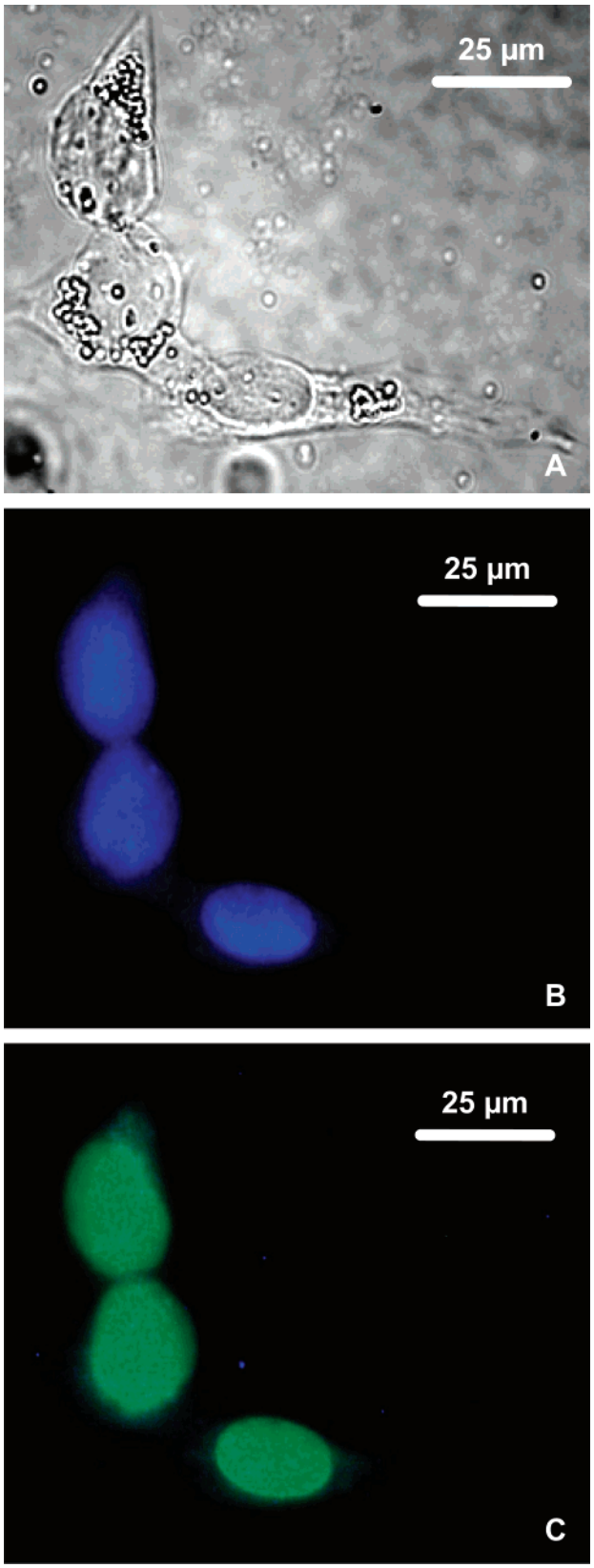

Figure 1. Intracellular localization of antisense oligonucleotides. Typical images of A2780 human ovarian carcinoma cells incubated for 48 h with FITC-labeled ASO in liposomes targeted to HIF1A mRNA: (A) light microscopy, (B) fluorescence microscopy with Hoechst 33258 nuclear staining, and (C) fluorescence microscopy with FITC-labeled ASO.

(22) Dharap, S. S.; Minko, T. Targeted proapoptotic LHRH-BH3 peptide. *Pharm. Res.* **2003**, *20*, 889−896.
(23) Dharap, S. S.; Qiu, B.; Williams, G.; Sinko, P.; Stein, S.; Minko, T. Molecular targeting of drug delivery systems to ovarian cancer by BH3 and LHRH peptides. *J. Controlled Release* **2003**, *91*, 61−73.

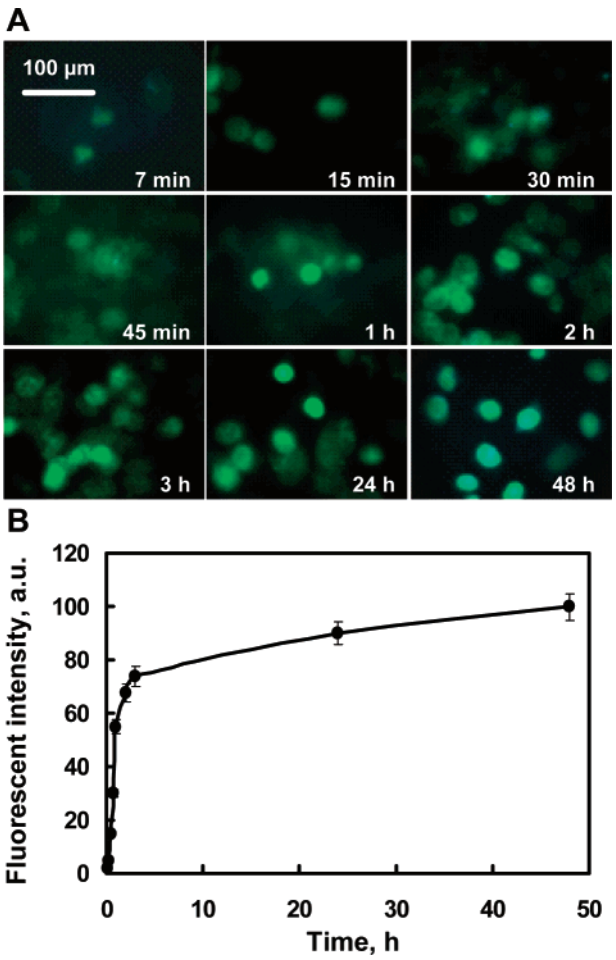

Figure 2. Intracellular release of FITC-labeled ASO from liposomes. (A) Typical images of A2780 human ovarian carcinoma cells incubated for different periods of time with FITC-labeled ASO in liposomes targeted to HIF1A mRNA. (B) Time course of the fluorescence intensity of FITC-labeled ASO released from liposomes. Means ± SD from four independent measurements are shown.

Results

Intracellular Localization and Release of Liposomal HIF1A Antisense Oligonucleotides. Analysis of intracellular localization of FITC-labeled ASO by fluorescent microscopy showed that oligonucleotides released from liposomes accumulated in cell nuclei (Figure 1). A superimposition of light and fluorescent pictures obtained using excitation wavelengths corresponding to Hoechst 33258 (nuclear stain) and FITC (ASO stain) on the same cells clearly supports such a conclusion. The fluorescence of labels inside micelles or liposomes in an aqueous solution is known to be strongly quenched by the outer shells of the micellar or liposomal formation.[17] Therefore, the absence of visible fluorescence in the cytosol suggests that fluorescent molecules associated with ASO are transferred within a pinocytic−endosomic vesicle to the nucleus. In contrast, free fluorescent ASO do not enter cells even when they are used at the highest attainable concentration (~1 mg/mL, data not shown).

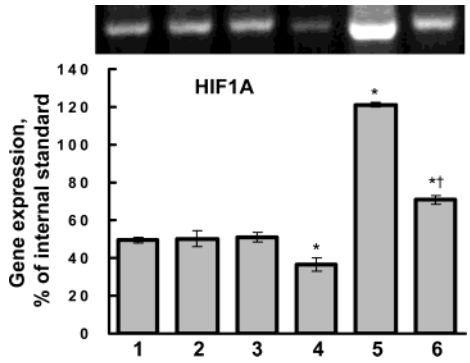

Figure 3. Typical images of the gel electrophoresis of RT-PCR products and expression of the *HIF1A* gene (percentage of the internal standard, β_2-microglobulin) in A2780 human ovarian carcinoma cells. Means ± SD from four independent measurements are shown: (1) control, normoxia, no treatment; (2) normoxia, empty liposomes; (3) normoxia, liposomal HIF1A sense oligonucleotides; (4) normoxia, liposomal HIF1A ASO; (5) hypoxia, no treatment; and (6) hypoxia, liposomal HIF1A ASO. An asterisk denotes a P of <0.05 when compared with control (normoxia). A dagger denotes a P of <0.05 when compared with hypoxia without treatment.

Nearly 70% of the fluorescence could be detected within the cells in the first three hours. By the 48th hour, nearly 100% of the fluorescence was localized within the nuclei (Figures 1 and 2). A series of *in vitro* experiments established the stability of the liposomes containing fluorescent ASO. Liposomes incubated in saline for several weeks did not release any significant amount of labeled ASO.

Liposomal ASO Targeted to HIF1A mRNA Significantly Weakened the Effects of Hypoxia on the Expression of Hypoxia Inducible Factor 1α and von Hippel-Lindau Tumor Suppressor Protein. The measurement of the level of expression of the targeted *HIF1A* gene showed that liposomal ASO targeted to this gene led to significant downregulation of the expression (Figure 3). This effect was more pronounced under hypoxic conditions. In fact, liposomal ASO decreased the level of expression of the targeted *HIF1A* gene by 1.4- and 1.7-fold in normoxia and hypoxia, respectively. In contrast, empty liposomes and liposomes containing oligonucleotides with the sequence corresponding to the sense strand of mRNA (SO) did not significantly change the expression of the *HIF1A* gene in both normoxia and hypoxia (Figure 3, bars 2 and 3). Therefore, liposomal ASO targeted against HIF1A mRNA significantly limited the overexpression of the targeted gene under hypoxia. Western blot analysis of the expression of HIF1A confirmed the RT-PCR data and showed that liposomal ASO targeted to HIF1A significantly limited the expression of this protein in both normoxia and hypoxia (Figure 4).

The analysis of the expression of the von Hippel-Lindau tumor suppressor gene product (VHL) showed that the liposomal ASO-directed *HIF1A* gene decreased the level of expression of the *VHL* gene in normoxia (Figure 5). Hypoxia alone significantly downregulated the expression of this gene. Liposomal ASO substantially limit this effect of hypoxia;

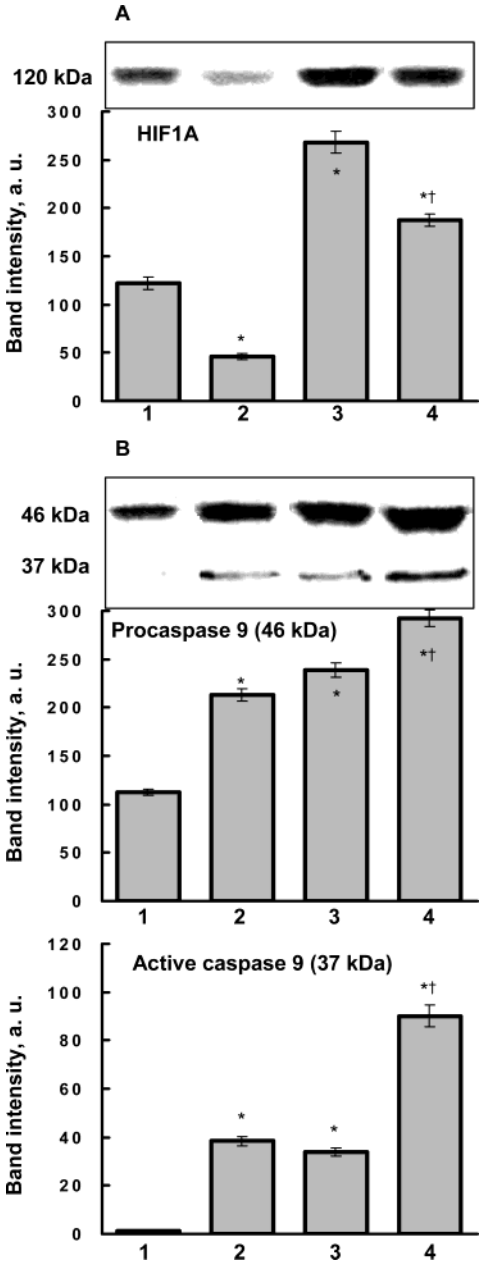

Figure 4. Typical images of Western blots of HIF1A (A) and caspase 9 (B) proteins and densitometric analysis of bands. Band intensities are shown in arbitrary units. Means ± SD from four independent measurements are shown: (1) control, normoxia, no treatment; (2) normoxia, liposomal HIF1A ASO; (3) hypoxia, no treatment; and (4) hypoxia, liposomal HIF1A ASO. An asterisk denotes a *P* of <0.05 when compared with control (normoxia). A dagger denotes a *P* of <0.05 when compared with hypoxia without treatment.

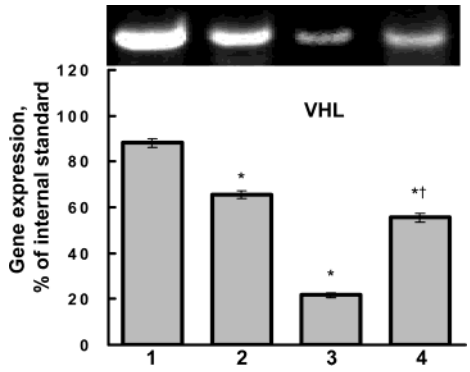

Figure 5. Typical images of gel electrophoresis of RT-PCR products and expression of the *VHL* gene (percentage of the internal standard, β_2-microglobulin) in A2780 human ovarian carcinoma cells. Means ± SD from four independent measurements are shown: (1) control, normoxia, no treatment; (2) normoxia, liposomal HIF1A ASO; (3) hypoxia, no treatment; and (4) hypoxia, liposomal HIF1A ASO. An asterisk denotes a *P* of <0.05 when compared with control (normoxia). A dagger denotes a *P* of <0.05 when compared with hypoxia without treatment.

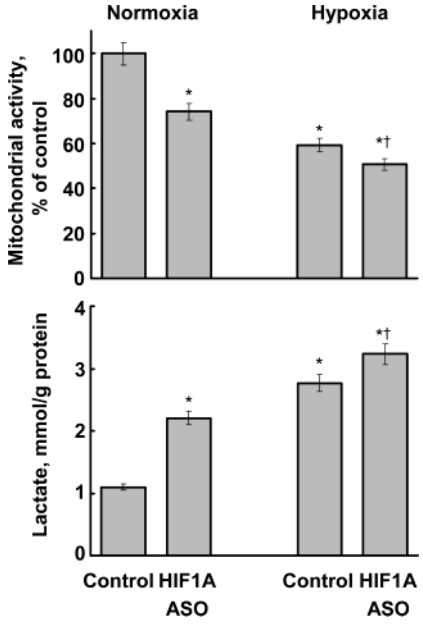

Figure 6. Mitochondrial activity and lactate accumulation in A2780 human ovarian carcinoma cells. Means ± SD from eight independent measurements are shown.

therefore, after the action of ASO under the hypoxic conditions, the level of expression of the *VHL* gene was substantially higher when compared with the level with hypoxia alone.

Liposomal ASO Targeted to HIF1A mRNA Induced Cellular Hypoxia. To characterize cellular aerobic and anaerobic metabolism, we measured mitochondrial activity by the MTT assay and lactate accumulation in cellular lysates (Figure 6). As expected, hypoxia downregulated oxidative and activated anaerobic cellular metabolism, leading to lactate accumulation. The degree of suppression in mitochondrial respiration was proportional to the degree of lactate accumulation. Unexpectedly, incubation of cancer cells with liposomes containing antisense oligonucleotides against HIF1A mRNA led to the statistically significant suppression of aerobic and activation of anaerobic metabolism. This effect was considerably more pronounced in normoxia than in hypoxia. Empty liposomes and liposomes containing sense oligonucleotides did not produce statistically significant

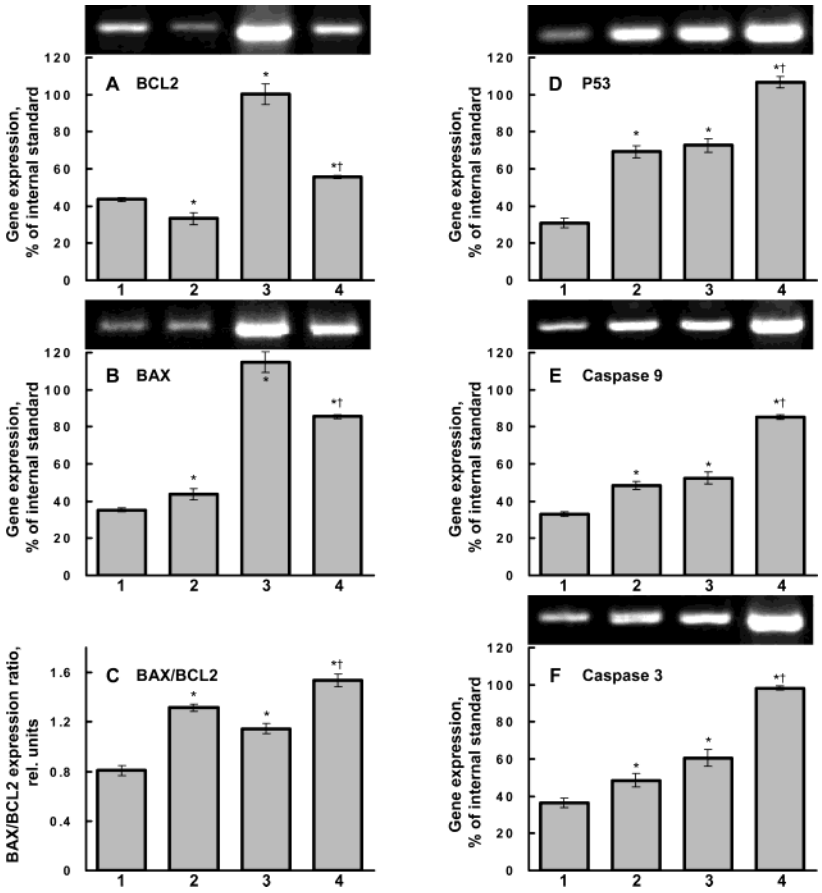

Figure 7. Typical images of gel electrophoresis of RT-PCR products and expression of genes (percentage of the internal standard, β_2-microglobulin) encoding BCL2 (A), BAX (B), and P53 (D) proteins, caspases 9 (E) and 3 (F), and BAX:BCL2 (C) expression ratios in A2780 human ovarian carcinoma cells. Means ± SD from four independent measurements are shown: (1) control, normoxia, no treatment; (2) normoxia, liposomal HIF1A ASO; (3) hypoxia, no treatment; and (4) hypoxia, liposomal HIF1A ASO. An asterisk denotes a P of <0.05 when compared with control (normoxia). A dagger denotes a P of <0.05 when compared with hypoxia without treatment.

changes in both aerobic and anaerobic cellular metabolism (data not shown).

Downregulation of the Expression of the HIF1A Gene Induced the Mitochondria-Mediated Apoptotic Cell Death Signal and Suppressed Antiapoptotic Resistance. To study the influence of liposomal ASO targeted to HIF1A mRNA on the cellular resistance and mitochondria-mediated cell death signal, we analyzed the expression of *BCL2* and BAX genes, the main players in the antiapoptotic cellular resistance and mitochondrial cell death signal, respectively[24−26] (Figure 7). Under the normoxia conditions, liposomal ASO targeted to HIF1A significantly decreased the level of *BCL2* expression. A simultaneous increase in the level of expression of the *BAX* gene led to the marked increase in the BAX:BCL2 ratio which is an index of the mitochondria-mediated apoptotic cell death signal.[27] Exposure of human ovarian cancer cells to hypoxia significantly activated the apoptotic cell death signal by the upregulation of *BAX* gene expression. However, hypoxia simultaneously overexpressed the *BCL2* gene, activating cellular antiapoptotic defense. As a result, the increase in the BAX:BCL2 ratio was limited and the degree of the increase was less pronounced when compared with that of HIF1A ASO in normoxia. Application of liposomal HIF1A ASO under hypoxic conditions significantly limited the overexpression of the *BCL2* and to a lesser extent the expression of the *BAX* genes. As the result, the BAX:BCL2 ratio was substantially higher after application of liposomal HIF1A ASO in hypoxia than with hypoxia alone (compare bars 3 and 4 in Figure 7).

Prevention of Hypoxic Overexpression of the *HIF1A* Gene Strengthened the Ability of Hypoxia To Induce P53

(24) Lowe, S. W.; Lin, A. W. Apoptosis in cancer. *Carcinogenesis* **2000**, *21*, 485−495.

(25) Oltvai, Z. N.; Milliman, C. L.; Korsmeyer, S. J. Bcl-2 heterodimerizes in vivo with a conserved homolog, Bax, that accelerates programmed cell death. *Cell* **1993**, *74*, 609−619.

(26) Reed, J. Dysregulation of apoptosis in cancer. *J. Clin. Oncol*. **1999**, *17*, 2941−2953.

(27) Takagi-Morishita, Y.; Yamada, N.; Sugihara, A.; Iwasaki, T.; Tsujimura, T.; Terada, N. Mouse uterine epithelial apoptosis is associated with expression of mitochondrial voltage-dependent anion channels, release of cytochrome C from mitochondria, and the ratio of Bax to Bcl-2 or Bcl-X. *Biol. Reprod.* **2003**, *68*, 1178−1184.

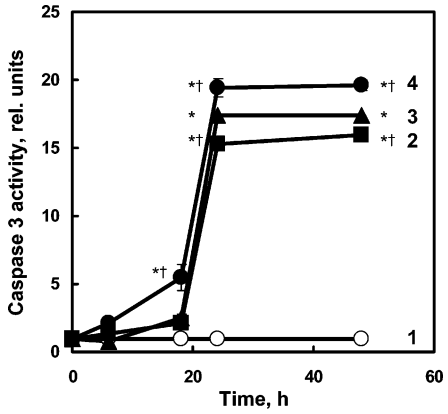

Figure 8. Time-dependent activity of caspase 3 in A2780 human ovarian carcinoma cells. Activities in the control (untreated cells) were set to a relative unit of 1. Means ± SD from four independent measurements are shown: (1) control, normoxia, no treatment; (2) normoxia, liposomal HIF1A ASO; (3) hypoxia, no treatment; and (4) hypoxia, liposomal HIF1A ASO. An asterisk denotes a P of <0.05 when compared with control (normoxia). A dagger denotes a P of <0.05 when compared with hypoxia without treatment.

and Caspase-Dependent Pathway of Apoptosis. We found that in addition to the activation of the mitochondria-mediated cell death signal, both hypoxia and ASO targeted to HIF1A mRNA also triggered the cell death signal by the overexpression of the *P53* gene (Figure 7). Therefore, it was not surprising that antisense oligonucleotides targeted to HIF1A themselves induced cell death by overexpressing genes encoding caspases and demonstrated synergism with hypoxia promoting hypoxic induction of the caspase-dependent cell death pathway. We found that liposomal HIF1A ASO and hypoxia not only activated procaspase 9 but also converted inactive caspase 9 to its active form (Figure 4). Active caspase 9 triggers a cascade of downstream caspases, which in turn lead to induction of apoptosis.[28]

Direct measurement of the activity of the main apoptosis executor, caspase 3, showed that both hypoxia and liposomal ASO targeted to HIF1A mRNA significantly activated this caspase (Figure 8, compare line 1 with lines 2 and 3). This activation began after approximately 20 h of hypoxic exposure and quickly reached the plateau starting from 24 h. It is interesting that the application of liposomal HIF1A ASO alone in normoxia led to caspase 3 activation, which was only slightly less pronounced than those in hypoxia (in Figure 8, compare lines 2 and 3). Suppression of the expression of the HIF1A gene under hypoxic conditions further activated the caspase (in Figure 8, compare line 4 with lines 2 and 3).

The Modulation of Antiapoptotic Cellular Resistance by the Suppression of HIF1A Enhanced the Ability of

(28) Minko, T.; Kopeckova, P.; Kopecek, J. Preliminary evaluation of caspase-dependent apoptosis signaling pathways of free and HPMA copolymer-bound doxorubicin in human ovarian carcinoma cells. *J. Controlled Release* **2001**, *71*, 227−237.

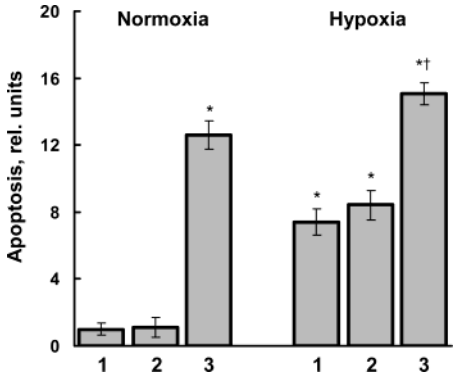

Figure 9. Apoptosis induction in human ovarian carcinoma cells. The enrichment of histone-associated DNA fragments (mono- and oligonucleosomes) in control cells was set to 1 unit, and the degree of apoptosis was expressed in relative units. Means ± SD from four independent measurements are shown: (1) control, no treatment; (2) empty liposomes; and (3) liposomal HIF1A ASO. An asterisk denotes a P of <0.05 when compared with control (normoxia). A dagger denotes a P of <0.05 when compared with hypoxia without treatment.

Hypoxia To Induce Apoptosis. Apoptosis was assessed by two independent methods. The first approach was based on measuring the enrichment of histone-associated DNA fragments (mono- and oligonucleosomes) in the cell cytoplasm using anti-histone and anti-DNA antibodies. The second approach was based on the detection of single- and double-stranded DNA breaks (nicks) using the terminal deoxynucleotidyl transferase-mediated dUTP-fluorescein nick end labeling (TUNEL) method. The results are presented in Figures 9 and 10. Both methods of apoptosis detection showed that hypoxia induced apoptosis in cancer cells. Liposomal ASO targeted to HIF1A mRNA was also able to induce apoptosis in normoxia. It is interesting that the degree of apoptosis induction by liposomal HIF1A ASO in normoxia was significantly higher than that induced by hypoxia alone. Further investigation showed that the downregulation of the expression of the HIF1A gene strengthened the ability of hypoxia to induce apoptosis in human ovarian cancer cells by simultaneous activation of cell death signaling pathways and suppression of cellular antiapoptotic resistance. In contrast, empty liposomes did not lead to significant apoptosis induction in normoxia and did not influence the induction of apoptosis by hypoxia.

Discussion

Our data show that a relatively simple liposomal drug delivery system can be used to substantially enhance the ability of antisense nucleotides to transfect cancer cells and decrease the level of expression of the targeted gene and protein. Analysis of the intracellular localization of the fluorescently labeled ASO by fluorescence microscopy led to the conclusion that liposomes containing ASO were most probably internalized by endocytosis followed by their transport in endosomes. This explains why we did not observe measurable levels of ASO fluorescence in the

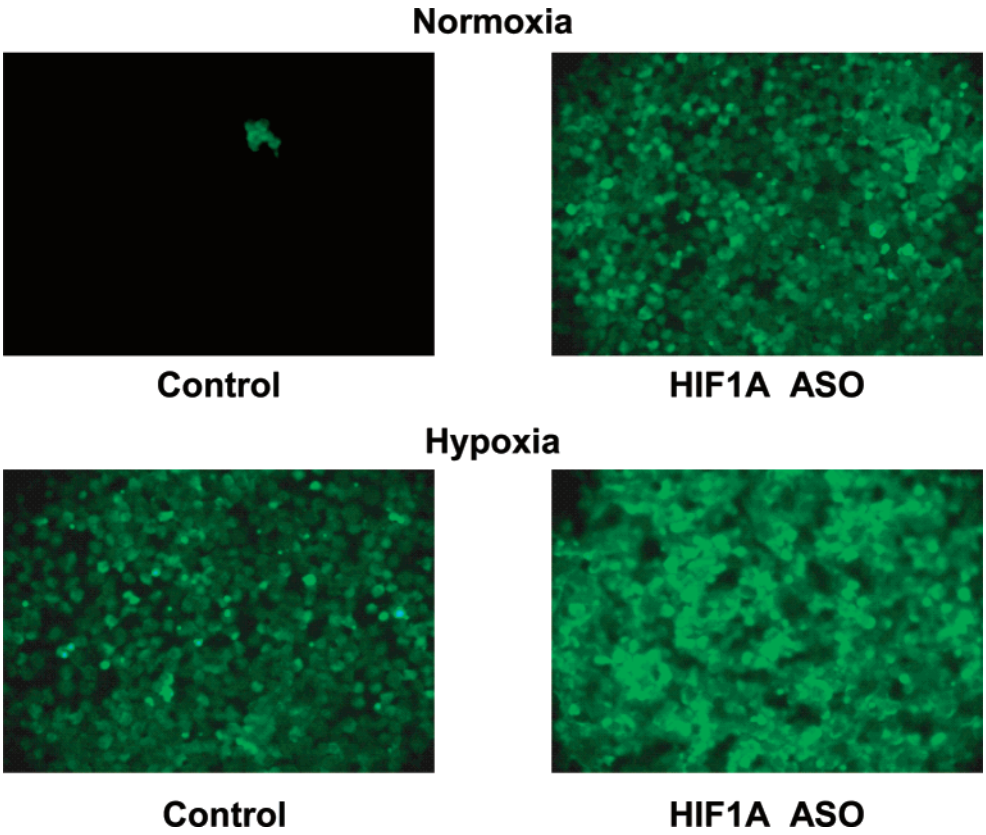

Figure 10. Typical fluorescence microscopy images of TUNEL-labeled A2780 human ovarian carcinoma cells.

cellular cytoplasm. Indeed, if ASO were transferred within the cell in intact liposomes, the fluorescence of their label would be quenched by the liposomal membranes. In this study, images from fluorescence microscopy indicate that the labeled ASO are transferred from the liposomes by a pinocytic−endosomic−lysosomic transfer to the perinuclear region, which is similar to that reported for polymer-bound active substances.[29,30] This process of delivery of ASO to the perinuclear region provides for an efficient suppression of the targeted mRNA (HIF1A). In contrast, liposomes used in this study were highly stable and did not release significant amounts of ASO during a several week incubation in saline.

Analysis of the data that were obtained showed that HIF1 has a bimodal role in cellular responses to hypoxia. On one hand, the activation of this protein by hypoxia triggers apoptotic and necrotic cell death pathways (Figure 11). Three main processes play major roles in these pathways. First, hypoxia may activate apoptosis through HIF1A-mediated overexpression of the P53 protein, which in turn activates BAX, a proapoptotic member of the BCL2 protein family.[13] Second, oxygen deficiency limits aerobic metabolism and, through the HIF1A transcription factor, leads to the compensatory increase in anaerobic metabolism. Third, hypoxia activates phospholipases and lipid peroxidation which in turn leads to the disturbances in membrane lipid composition and an increase mitochondrial membrane permeability.[1] Activation of BAX protein and the increase in the permeability of the mitochondrial membrane provoke the release of cytochrome *c* into the cytoplasm. This release in turn activates a series of events that leads to the activation of caspases and apoptotic cell death. The limitation of aerobic metabolism and activation of anaerobic glycolysis and associated lactate acidosis, metabolic derangement (including ATP insufficiency), and injury are the main causes of necrotic cell death (Figure 11). On the other hand, hypoxia through the activation of the HIF1 transcriptional factor strengthens the cellular antiapoptotic defense and improves mitochondrial respiration and the stability of its membranes by the overexpression of the BCL2 protein. These processes substantially limit apoptotic cell death induced by hypoxia. Moreover, such adaptive effects of hypoxia developed in tumors lead to an increase in the resistance of cancer cells to different types of cancer therapy.[7,31]

Our data show that in cancer cells the balance between these two processes, damaging and protective effects of hypoxia, slightly favors the induction of cell death. We hypothesize that to release the potential of hypoxia to induce

(29) Kopecek, J.; Kopeckova, P.; Minko, T.; Lu, Z. HPMA copolymer-anticancer drug conjugates: design, activity, and mechanism of action. *Eur. J. Pharm. Biopharm.* **2000**, *50*, 61−81.

(30) Minko, T.; Dharap, S. S.; Pakunlu, R. I.; Wang, Y. Molecular targeting of drug delivery systems to cancer. *Curr. Drug Targets*, in press.

(31) Shannon, A. M.; Bouchier-Hayes, D. J.; Condron, C. M.; Toomey, D. Tumour hypoxia, chemotherapeutic resistance and hypoxia-related therapies. *Cancer Treat. Rev.* **2003**, *29*, 297−307.

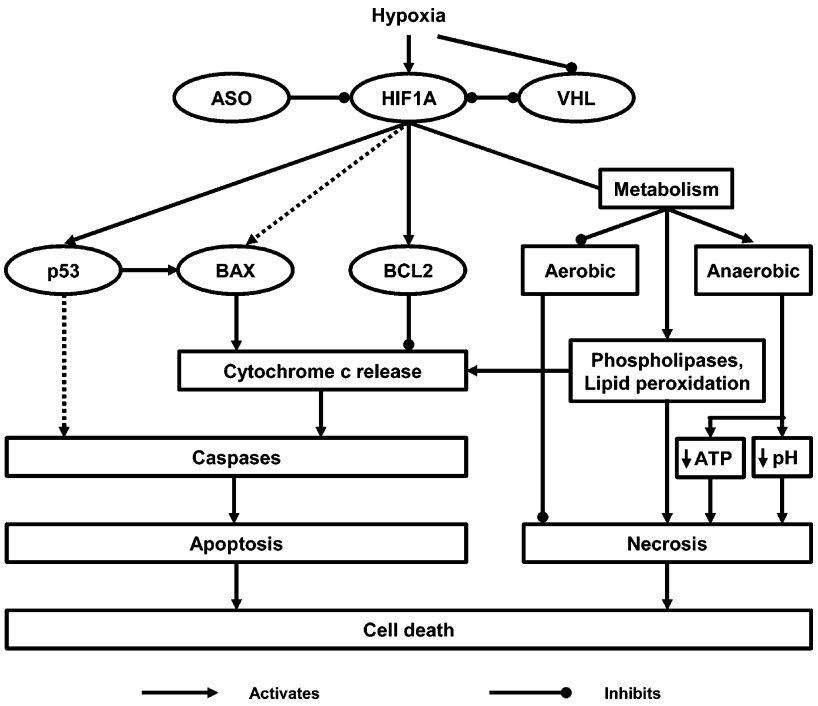

Figure 11. Scheme showing the bimodal effect of hypoxia in cancer cells.

cell death to a full extent and prevent the development of antiapoptotic resistance in cancer cells, this balance should be further shifted toward apoptotic death by the partial suppression of the overexpression of HIF1A. Our data support this hypothesis and show that downregulation of the expression of this protein by liposomal ASO targeted to HIF1A mRNA significantly weakens the cellular antiapoptotic defense, promotes cell death signaling associated with BAX protein, and even further increases the magnitude of the P53-mediated cell death signal. Finally, this leads to a significant increase in the level of cell death in both normoxia and hypoxia. Data obtained in this study also show that an induction of cell death by hypoxia requires significantly less expression of HIF1A protein, while activation of protective effects needs a significantly higher level of expression of HIF1A. This unexpected result is supported by experimental data presented here which show that partial inhibition of HIF1A expression almost completely prevents the activation of antiapoptotic cellular defense and had an insignificant effect on proapoptotic processes. These results demonstrate that HIF1A might be an attractive therapeutic target for anticancer therapy. Therefore, ASO targeted to HIF1A mRNA might be used alone or in combination with other treatments (radiation, chemotherapy, etc.) to increase the level of cancer cell death, prevent the development of cellular resistance, and therefore increase the efficacy of cancer therapy.

MP034031N